PHYSICAL REVIEW B VOLUME 52, NUMBER 7 15 AUGUST 1995-I

Chemisorption of Li on jellium: Local density of states and nuclear-spin relaxation

W. Mannstadt* and G. Grawert
Fachbereich Physik der Philipps-Universität Marburg, 35032 Marburg Renthof 6, Germany

(Received 7 December 1994; revised manuscript received 13 February 1995)

Nuclear-spin relaxation of atoms chemisorbed on metal surfaces is investigated theoretically. The underlying interaction is the Fermi contact interaction between the magnetic moments of the nucleus and the surrounding electrons. In a resulting rate equation for the nuclear polarization, the rate depends on the local density of electron states (LDOS) at the nuclear site. This LDOS is calculated in the framework of density-functional theory via solving Dyson's equation using the jellium model for the metal substrate. The model results are consistent with the data.

I. INTRODUCTION

Investigations of the properties of solid surfaces and of adsorption of atoms on surfaces are important because of their technological relevance. One of the relevant problems concerns the electronic structure.[1] Global as well as local structures are of interest. An adsorbed atom gives rise to an induced density of electron states altering the band structure of the clean substrate. The local density of states (LDOS) at the position of the nucleus contains information on the functional dependence of the electronic structure on both energy and geometric site. In addition to classical methods in surface physics, recently chemisorption phenomena have been investigated with nuclear-spin-polarized nuclei.[2–4] The detection of the decay rate of an initial spin polarization of the adsorbed atom provides information on the chemisorption process. Through the decay rate one measures the LDOS at the position of the adatom nucleus at the Fermi energy.

Experimental studies with polarized nuclei are well established in the field of NMR. A variety of experimental and theoretical investigations of the nuclear magnetic relaxation of nuclei implanted in solids have been performed. From the hyperfine interaction of the nucleus with the bulk electrons, information on the local electronic structure is obtained. In NMR literature this relaxation process is known as spin-lattice relaxation.[5,6] Nuclear-spin relaxation of atoms chemisorbed on surfaces has been measured for polarized Li on a variety of metal surfaces, and recently also on Si.

The approach which we put forward is devised to capture the essential physics touched by the relaxation rate and its main ingredient, the LDOS. Therefore the present paper starts from simple physical pictures, using the jellium model to describe the substrate.

In Sec. II A we present a brief summary of the time development of an ensemble of nuclei in the presence of an electronic surrounding. The interaction thereby considered is the Fermi contact interaction, since in most cases this represents the dominant interaction. As a result one obtains a rate equation for the polarization which under normal conditions exhibits an exponential decay of the polarization with a rate proportional to the temperature and the LDOS.

In Sec. II B a method for calculating the LDOS of a chemisorbed atom is put forward. The density-functional theory and especially Dyson's equation for the Green's function is applied to calculate the LDOS at the position of the nucleus. To obtain insight into the essential physics involved, the chemisorption of Li atoms on a jellium surface is studied. Results for the induced density of states are discussed in Sec. III. Also, the spatial electron density in the vicinity of the chemisorbed atom is calculated. Finally a discussion of the relaxation rate obtained for Li on several jellium surfaces, and a comparison with experimental data, are presented. Section IV gives a summary and conclusion.

II. THEORY

A. Rate equation

To describe the polarization of an ensemble of particles with spin I, one usually refers to the density matrix in spin space. Expanding the density matrix in a set of irreducible tensor operators $\tau_{k,q}$ one obtains a description of the polarization in terms of spherical polarization parameters $t_{k,q}$:[7]

$$\rho=\sum_{k,q} t_{k,q}\tau^{\dagger}_{k,q}\ ,$$
$$t_{k,q}=\mathrm{Tr}\,\tau_{k,q}\rho\ ,\quad k=0,1,\ldots,2I\ ,\quad -k\le q\le k\ . \tag{1}$$

The tensor operators $\tau_{k,q}$ are defined by their matrix elements in spin space:

$$\langle I,m'|\tau_{k,q}|I,m\rangle=\sqrt{2k+1}\langle I,m'|I,m;k,q\rangle\ . \tag{2}$$

where $\langle\ \rangle$ is a Clebsch Gordan coefficient. The time dependence of the polarization in the Schrödinger picture is then given by

$$\dot{t}_{k,q}=\mathrm{Tr}\,\tau_{k,q}\dot{\rho}\ . \tag{3}$$

Because we are interested in a relaxation process due to a change of the population of the magnetic sublevels (T_1 times in NMR), only the diagonal matrix elements of the density matrix ρ and consequently the parameters $t_{k,0}$ are relevant. Therefore a second relaxation time T_2, well know in other publications,[5,6] does not occur in the present problem.

The interaction between the nucleus of the atom and the metal surface to be considered here is the Fermi contact interaction, i.e., the interaction of the magnetic moment of the nucleus with the magnetic field produced by the electrons at the position of the nucleus.[8] In most cases this is the dominant part of the interaction:

$$H_{\mathrm{int}}=-\boldsymbol{\mu}\cdot\mathbf{B}_{\mathrm{el}}(\mathbf{r}_N)=-\frac{\mu_0}{4\pi}\frac{8\pi}{3}g_{\mathrm{el}}g_N\mu_{\mathrm{el}}\mu_N\mathbf{S}_{\mathrm{el}}(\mathbf{r}_N)\cdot\mathbf{I}\ . \qquad (4)$$

Here $\mathbf{S}_{\mathrm{el}}(\mathbf{r}_N)$ represents the electron-spin density at the position of the nucleus and $g_{\mathrm{el}},g_N,\mu_B,\mu_N$ are the g factors, the Bohr magneton, and the nuclear magneton. Throughout this paper the Système International (SI)-system of units is used, and μ_0 is the vacuum permeability. $\mathbf{S}$ and $\mathbf{I}$ are the dimensionless spin operators. This interaction Hamiltonian describes a coupling between the nuclear spin of the chemisorbed atom and the substrate. To define an axis of quantization (which is chosen to be the z axis) an external magnetic field B_0 is applied. In the NMR literature, the theoretical treatment of this so-called spin-lattice relaxation is well known: An exponential decay of the initial nuclear polarization is obtained:[5,6,9,10]

$$\dot{t}_{k,0}=-\alpha_k t_{k,0}\ ,$$

$$\alpha_k=-\frac{k(k+1)}{2}\left[\frac{\mu_0}{4\pi}\frac{8\pi}{3}g_{\mathrm{el}}g_N\mu_{\mathrm{el}}\mu_N\right]^2\frac{1}{\hbar}\coth\frac{\hbar\omega_0}{2k_BT}$$
$$\times\mathrm{Im}_{\chi_{-1,1}}(\mathbf{r}_N,\mathbf{r}_N,\omega_0)\ , \qquad (5)$$

where k_B, T, and ω_0 are the Boltzmann factor, the temperature of the substrate, and the Larmor frequency of the nucleus. $\mathbf{r}_N$ is the position of the nucleus. For further detail see, e.g., Refs. 5 and 6.

For temperatures around 1000 K, which are of interest here, and a magnetic-field strength of less than 1 T, one has $(\hbar\omega_0/2k_BT)\approx10^{-7}$. The approximation of $\coth x\approx(1/x)$ therefore holds, and the equation for α_k reads

$$\alpha_k=-\frac{k(k+1)}{2}\left[\frac{\mu_0}{4\pi}\frac{8\pi}{3}g_{\mathrm{el}}g_N\mu_{\mathrm{el}}\mu_N\right]^2\frac{1}{\hbar}\frac{2k_BT}{\hbar\omega_0}$$
$$\times\mathrm{Im}\chi_{-1,1}(\mathbf{r}_N,\mathbf{r}_N,\omega_0)\ . \qquad (6)$$

The spin susceptibility is calculated in the independent particle approximation, which gives the following expression for $\chi_{-1,1}$:

$$\chi_{-1,1}(\mathbf{r},\mathbf{r}',\omega)=\tfrac{1}{2}\sum_{\mu,\nu}\phi_\mu^*(\mathbf{r}')\phi_\nu(\mathbf{r}')\phi_\nu^*(\mathbf{r})\phi_\mu(\mathbf{r})$$
$$\times\frac{f_\nu(\frac{1}{2})-f_\mu(-\frac{1}{2})}{\hbar\omega-(E_{\mu,-(1/2)}-E_{\nu,(1/2)})+i\epsilon}\ , \qquad (7)$$

with

$$f_\mu(m_s)=\frac{1}{1+\exp\beta(E_\mu+m_s2\mu_BB_0-E_F)}\ ,$$

where the chemical potential is approximated by the Fermi energy. Using the spectral representation for the Green's function,

$$G^+(\mathbf{r}',\mathbf{r},E)=\sum_\mu\frac{\phi_\mu^*(\mathbf{r}')\phi_\mu(\mathbf{r})}{E-E_\mu+i\epsilon}\ , \qquad (8)$$

one finds the following expression for the susceptibility:

$$\chi_{-1,1}(\mathbf{r},\mathbf{r}',\omega)=\tfrac{1}{2}\sum_\nu f_\nu\tfrac{1}{2}\phi_\nu^*(\mathbf{r})\phi_\nu(\mathbf{r}')[G^+(\mathbf{r}',\mathbf{r},E_\nu+2\mu_BB_0+\hbar\omega)]+f_\nu(-\tfrac{1}{2})\phi_\nu^*(\mathbf{r}')\phi_\nu(\mathbf{r})[G^+(\mathbf{r}',\mathbf{r},E_\nu-2\mu_BB_0-\hbar\omega)]^*\ . \qquad (9)$$

Replacing the sum over the discrete states into an integral over the density of energy states, the susceptibility for $\mathbf{r}=\mathbf{r}'$ reads

$$\chi_{-1,1}(\mathbf{r},\mathbf{r},\omega)=-\frac{1}{2\pi}\left\{\int dE\,f(E)\mathrm{Im}G^+(\mathbf{r},\mathbf{r},E-\mu_BB_0)[G^+(\mathbf{r},\mathbf{r},E+\mu_BB_+\hbar\omega]\right.$$
$$\left.+\int dE\,f(E)\mathrm{Im}G^+(\mathbf{r},\mathbf{r},E+\mu_BB_0)[G^+(\mathbf{r},\mathbf{r},E-\mu_BB_0-\hbar\omega]^*\right\}. \qquad (10)$$

Since $\hbar\omega_0$, which is only of interest for the relaxation process, is small compared to the energies in the solid, first-order expansion in $\hbar\omega$ for the imaginary part of the susceptibility yields

$$\mathrm{Im}\chi_{-1,1}(\mathbf{r},\mathbf{r},\omega_0)$$
$$=+\frac{\hbar\omega_0}{2\pi}\int dE\left[\frac{\partial}{\partial E}f(E)\right]\mathrm{Im}G^+(\mathbf{r},\mathbf{r},E-\mu_BB_0)$$
$$\times\mathrm{Im}G^+(\mathbf{r},\mathbf{r},E+\mu_BB_0)\ . \qquad (11)$$

The derivative of the Fermi function has a sharp peak at the Fermi energy. Replacing it by a δ function peaked a the Fermi energy, and neglecting the energy splitting of the electron states in an external magnetic field, one finds

$$\mathrm{Im}\chi_{-1,1}(\mathbf{r},\mathbf{r},\omega_0)=-\frac{\hbar\omega_0}{2\pi}[\mathrm{Im}G^+(\mathbf{r},\mathbf{r},E_F)]^2\ . \qquad (12)$$

Since we are dealing with Fermi contact interaction only the susceptibility at the position of the nucleus, which is chosen to be the origin of the coordinate system, is needed. Thus the relaxation rate α_k is given by

$$\alpha_k=\frac{k(k+1)}{2}\left[\frac{16\pi}{3}\frac{\mu_0}{4\pi}\mu_N\mu_B\right]^2\frac{1}{\hbar\pi}g_N^2k_BT\times[\mathrm{Im}G^+(0,0,E_F)]^2\ . \tag{13}$$

The expression $\mathrm{Im}G^+(\mathbf{r},\mathbf{r},E)$ is usually called the local density of states (LDOS). This result for the relaxation of a nuclear spin polarization is quite general. On the one hand thermodynamical effects result in a linear temperature dependence essentially over the whole temperature range since the expansion of $\coth(\hbar\omega_0/2k_BT)\approx(2k_BT/\hbar\omega_0)$ becomes wrong only for very low temperatures or strong magnetic fields. On the other hand, the local electronic structure surrounding the nucleus determines the relaxation behavior through the LDOS.

B. Local density of states

Subsequently the calculation of Green's function and the LDOS for chemisorbed atoms is briefly described.[9,10] State of the art electronic structure calculations are performed with the framework of the density-functional theory utilizing the local approximation for the exchange-correlation potential.[11–13] Thereby the Kohn-Sham equations have to be solved self-consistently:

$$\begin{aligned}&H_0\psi_i(\mathbf{r})=E_i\psi_i(\mathbf{r})\ ,\\&H_0=-\frac{\hbar^2}{2m}\Delta+V_{\mathrm{eff}}(\mathbf{r})\ ,\\&n(\mathbf{r})=\sum_i|\psi_i(\mathbf{r})|^2\ ,\\&V_{\mathrm{eff}}(\mathbf{r})=V_{\mathrm{xc}}(\mathbf{r})+\frac{e^2}{4\pi\epsilon_0}\int d^3r'\frac{n(\mathbf{r}')}{|\mathbf{r}-\mathbf{r}'|}+V_0(\mathbf{r})\ .\end{aligned}\tag{14}$$

Here V_0 represents the external potential from the positive nuclei of the system. $V_{\mathrm{xc}}(\mathbf{r})$ is the exchange-correlation potential. For the correlation potential the expression from Ceperley-Alder in the parametrization of Perdew-Zunger is used in the present paper.[14]

The Green's function of the system is defined through

$$G_0^+=\lim_{\epsilon\to0}\frac{1}{E-H_0+i\epsilon}\ . \tag{15}$$

From the Green's function one obtains the electron density

$$n_0(\mathbf{r})=-\frac{2}{\pi}\int_{-\infty}^{E_F}dE\ \mathrm{Im}G_0^+(\mathbf{r},\mathbf{r},E)\ . \tag{16}$$

where E_F is the Fermi energy of the system.

If in a first step the Green's function G_0 of the unperturbed substrate system is solved, the total Green's function can be calculated through Dyson's equation

$$G^\pm(E)=G_0^\pm(E)+G_0^\pm(E)\Delta VG^\pm(E)\ , \tag{17}$$

where ΔV is the change in the potential due to the chemisorbed atom:

$$\begin{aligned}\Delta V&=V_{\mathrm{eff}}(n_0(\mathbf{r})+\Delta n(\mathbf{r}))-V_{\mathrm{eff}}(n_0(\mathbf{r}))\\&=\Delta V_{\mathrm{xc}}(\mathbf{r})+\frac{e^2}{4\pi\epsilon_0}\int d^3r'\frac{\Delta n(\mathbf{r}')}{|\mathbf{r}-\mathbf{r}'|}-\frac{e^2}{4\pi\epsilon_0}\frac{Z}{r}\ ,\end{aligned}\tag{18}$$

$$\Delta V_{\mathrm{xc}}(\mathbf{r})=V_{\mathrm{xc}}(n_0(\mathbf{r})+\Delta n(\mathbf{r}))-V_{\mathrm{xc}}(n_0(\mathbf{r}))\ . \tag{19}$$

Defining the modification of Green's functions caused by the chemisorbed atom as

$$\Delta G^+(E)=G^+(E)-G_0^+(E)\ . \tag{20}$$

Dyson's equation for this difference of the two Green's functions is given by

$$\Delta G^+(E)=(1-G_0^+(E)\Delta V)^{-1}(G_0^+(E)\Delta VG_0^+(E))\ . \tag{21}$$

The difference in the electron density follows according to (16) from

$$\Delta n(\mathbf{r})=-\frac{2}{\pi}\int_{-\infty}^{E_F}dE\ \mathrm{Im}\Delta G^+(\mathbf{r},\mathbf{r},E)\ , \tag{22}$$

For the chemisorption, $\Delta n(\mathbf{r})$ is important because it reflects the change in the electron density due to the adsorbate.

Since a metal tends to screen out a perturbation, the region where $\Delta n(\mathbf{r})$ is different from zero is well localized. Therefore a rather small set of localized basis functions ϕ_i should be sufficient to describe $\Delta n(\mathbf{r})$.[15] The operator equation (21) then is solved as a matrix equation in the space of the appropriately chosen basis functions. Again a coupled system of equations has to be solved self-consistently:

$$\begin{aligned}&(\Delta G^+(E))_{i,j}=(1-G_0^+(E)\Delta)^{-1}_{i,k}(G_0^+(E))_{k,m}\\&\qquad\times(\Delta V)_{m,n}(G_0^+(E))_{n,j}\ ,\\&(\Delta n)_{i,j}=-\frac{2}{\pi}\int_{-\infty}^{E_F}dE\ \mathrm{Im}\Delta(G^+(E))_{i,j}\ ,\\&\Delta n(\mathbf{r})=\sum_{i,j}(\Delta n)_{i,j}\phi_i(\mathbf{r})\phi_j(\mathbf{r})\ ,\\&(\Delta V)_{i,j}=[V(n_0(\mathbf{r})+\Delta n(\mathbf{r}))]_{i,j}-[V(n_0(\mathbf{r}))]_{i,j}\ .\end{aligned}\tag{23}$$

After having solved these equations all the relevant information on the chemisorption can be deduced.

(1) The induced density of states $\Delta\rho(E)$:

$$\begin{aligned}\Delta\rho(E)&=-\frac{2}{\pi}\int d^3r\ \mathrm{Im}\Delta G^+(\mathbf{r},\mathbf{r},E)\\&=-\frac{2}{\pi}\sum_i(\mathrm{Im}\Delta G^+(E))_{i,i}\ .\end{aligned}$$

(2) The change in the electron density in the vicinity of the adsorbate:

$$\Delta n(\mathbf{r})=\sum_{i,j}(\Delta n)_{i,j}\phi_i(\mathbf{r})\phi_j(\mathbf{r})\ .$$

(3) The relaxation rate of the chemisorbed atom:

$$\alpha = c\left[\mathrm{Im}G_0^+(0,0,E_F) + \sum_{i,j}\phi_i(0)\phi_j(0)(\mathrm{Im}\Delta G^+(E_F))_{i,j}\right]^2 ,$$

cf. Eq. (13) for the factors in front of the bracket ($k=1$ for the case of ^{6}Li).

To investigate essential features of the physics determining the spin relaxation of chemisorbed atoms on a metal surface, calculations for the relaxation rate α were performed in the jellium model, i.e., the positive ions of the metal substrate atoms are replaced by a uniform positive background n_+.[16,17] Usually the parameter to characterize the jellium substrate is the Wigner Seitz radius r_s, which is related to the positive background density n_+ through

$$\frac{1}{n_+} = \frac{4\pi}{3}r_s^3 . \tag{24}$$

Thus by varying r_s different metal substrates are simulated. Choosing the z axis of the coordinate system as normal to the surface with a positive direction into the vacuum side, the positive background density has the form

$$n_+(\mathbf{r}) = \Theta(-z)n_+ . \tag{25}$$

Due to the axial symmetry around the z axis an appropriate ansatz for the Kohn-Sham eigenfunction is

$$\begin{aligned}
\psi_{E,k,m}(\mathbf{r}) &= \frac{1}{\sqrt{2\pi}}\sqrt{k_1}e^{im\varphi}J_m(k_1\rho)u_k(z) ,\\
E &= \frac{\hbar^2}{2m_e}(k_1^2+k^2) ,\\
\langle \psi_{E,k,m}|\psi_{E',k',m'}\rangle &= \delta(k_1-k_1')\delta(k-k')\delta_{m,m'} ,
\end{aligned} \tag{26}$$

where $u_k(z)$ are the numerical solution of the remaining Kohn-Sham equation in the variable z. From these eigenfunctions a Green's function is constructed via the spectral representation, which gives

$$\begin{aligned}
G_0^+(\mathbf{r},\mathbf{r}',E) &= -\frac{2m}{\hbar}\frac{1}{2\pi}\sum_m e^{im(\varphi-\varphi')}\int_{-\infty}^{+\infty} dk\, u_k^*(z)u_k(z') \times \begin{cases} I_m(\rho' c)K_m(\rho c) , & \rho'<\rho \\ I_m(\rho c)K_m(\rho' c) , & \rho<\rho' ,\end{cases}\\
c^2 &= k^2-\tilde{k}^2-i\epsilon , \quad \mathrm{Re}(c)>0 , \quad E=\frac{\hbar^2}{2m}\tilde{k}^2 .
\end{aligned} \tag{27}$$

Here K_m and I_m are modified Bessel functions. This expression for the Green's function G_0^+ is used in calculating the matrix elements in (21).

The basis functions in the vicinity of the adsorbate were chosen to be a Slater-type orbitals (STO) centered at the adatom nucleus:

$$\phi_i(\mathbf{r}) \overset{\wedge}{=} f_{\nu,l}(r)Y_{l,m}(\theta,\varphi) , \tag{28}$$

with

$$f_{\nu,l}(r) = Nr^{n-1}e^{-\zeta r} . \tag{29}$$

For the case of Li atoms a double-zeta (DZ) basis set is used. Since the chemisorption properties are dominated through the valence electrons the calculations were performed in the frozen-core approximation for the 1s electrons. That is, the basis functions for the 1s orbital of the Li atom are not varied and taken from the free atom. Furthermore s- and p-type orbitals were used to represent Δn. Therefore the basis consists of the following functions:

$$\chi_{1s}(\mathbf{r}) , \quad \chi_{1s'}(\mathbf{r}) , \quad \chi_{2s}(\mathbf{r}) ,$$

$$\chi_{2s'}(\mathbf{r}) , \quad \chi_{2p}(\mathbf{r}) , \quad \chi_{2p'}(\mathbf{r}) .$$

The exponentials ζ of the 2s and 2p orbitals are chosen to be identical in atomic units:[18]

$$\chi_{2s} \text{ and } \chi_{2p}\text{: } \zeta=1.97 ,$$

$$\chi_{2s'} \text{ and } \chi_{2p'}\text{: } \zeta'=0.67 .$$

The STO's of the 2s wave functions are orthogonalized with respect to the 1s wave function. Since the metal screens out the perturbation, the STO's are defined only within a sphere of radius R. The calculations showed that a radius of $R=3$ Å was sufficient.

III. RESULTS AND DISCUSSION

A. Induced density of states

Although the chemisorbed Li atom has an equilibrium distance d_{eq} from the surface of the substrate, which is determined by the energy minimum, it is interesting to study the dependence of various quantities on the distance of the Li atom from the jellium surface. First we investigate the induced density of states $\Delta\rho(E)$ for different distances d of the Li atom from the jellium surface. The distance d is measured from the position of the nucleus to the positive background n_+.

For an infinite distance of the Li atom from the surface the induced density of states equals that of the free atom, because there is no interaction between the surface and the atom. A treatment of the free atom is not possible within the framework of Sec. II B due to the fact that the density of states of a free atom consists of δ functions in energy, while in the self-consistent procedure a numerical integration with respect to the energy is required. Nevertheless for rather large distances a self-consistent solution is found.

In Fig. 1 the induced density of states is shown for three different distances of the Li atom. For the substrate

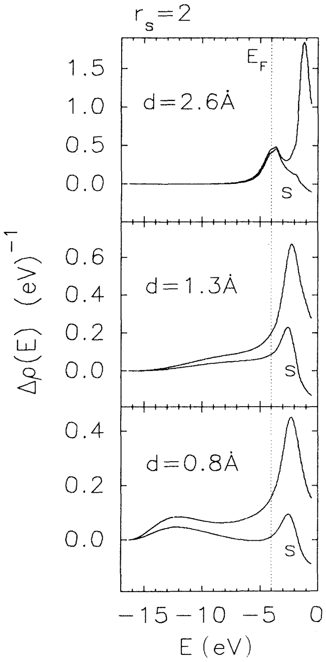

FIG. 1. The induced density of electron states for Li on a jellium substrate surface and its s-wave part for r_s of 2 bohr and three distances d of the Li nucleus from the surface. (The equilibrium distance is 1.3 Å.)

system the value of $r_s=2$ (bohr) was chosen, which corresponds to an Al surface. The energy is measured relative to the vacuum. Thus the bottom of the conduction band for this system lies at -16.3 eV. For large distances ($d=2.6$ Å) there are two sharp peaks in the induced density of states. An angular momentum decomposition of $\Delta\rho(E)$ shows that these peaks are well-separated states with s and p characters. Due to the weak interaction of the Li atom with the surface at these distances, one can identify these states with the atomic $2s$ and $2p$ states of Li. However, the states are shifted to higher energies. When the Li atom gets closer to the surface the increasing interaction broadens the sharp states into resonances, and both states are hybridized. The energetic separation of the $l=0$ and 1 parts of $\Delta\rho$ disappears. Both l states are spread over a wide energy range and have essentially the same shape. Pushing the Li atom further to the surface the induced density of states $\Delta\rho(E)$ again shows two maxima. Again the $l=0$ and parts have the same shape. This behavior of the induced density of states indicates a hybridization of the $2s$ and $2p$ states of the Li atom. For weak interaction the atomic character is dominant in $\Delta\rho(E)$. Due to the axial symmetry of the bare jellium potential a mixing of states with the same quantum number m of the angular momentum is possible. Therefore a hybridization of the $2s$ and $2p_z$ states occurs when the atom is moved closer to the surface. Projecting on the component of the angular momentum with $l=0$, one obtains two resonance peaks, which are most clearly seen for the distance $d=0.8$ Å.

The equilibrium distance for the adsorbed Li atom is found by minimizing the energy of the system. In Table I we give a summary of equilibrium distances for different values of r_s. For these equilibrium distances Fig. 2 shows the induced density of states $\Delta\rho(E)$. The conduction-band-width of the jellium system decreases with increasing r_s, since the positive background becomes smaller with increasing r_s. To demonstrate the influence of the conduction-band-width on the induced density of states $\Delta\rho(E)$, the energy range in all three plots is that of the jellium system with $r_s=2$ (bohr), which has the largest bandwidth. The Fermi energy E_F, the work function ϕ, and, for the systems with $r_s=3$ and 4 (bohr), the bottom of the band E_B is also marked.

For the jellium surface with $r_s=2$ (bohr) there is only one resonance in $\Delta\rho(E)$ above the Fermi energy. A decomposition of $\Delta\rho(E)$ into parts with $l=0$ and 1 shows that the s and p parts below the Fermi energy have the same shape, and that both are essentially of equal magnitude. For increased r_s the induced density of states $\Delta\rho(E)$ has two resonances which become the sharper the large the value of r_s. Moreover the resonance below the Fermi energy contains more and more s character. The system with $r_s=4$ (bohr) shows this result most clearly. This behavior of $\Delta\rho(E)$ is strongly influenced by the conduction-band-width. In systems with a small bandwidth there are less metal states that interact with the Li atom. Due to this weaker interaction the hybridization of the $2s$ and $2p$ states in the Li atom is reduced, leading to more atomiclike resonances.[19] With respect to the work function of the different systems, Fig. 2 gives the following result: The larger the work function of the sys-

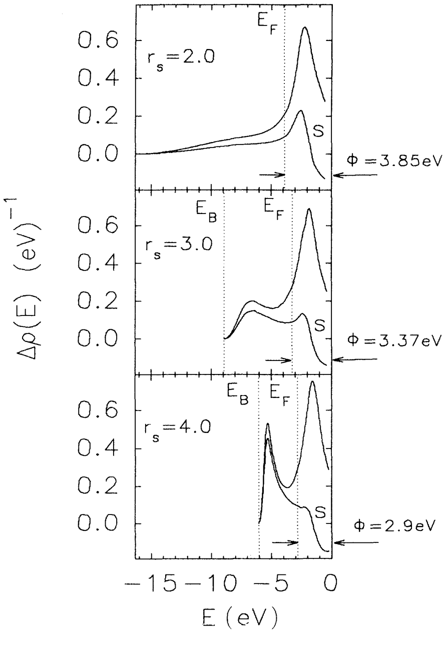

FIG. 2. The same as in Fig. 1, though for three different r_s and the respective equilibrium distances. E_B indicates the bottom of the conduction band, E_F the Fermi energy, and ϕ the work function. The energy is measured from the vacuum.

TABLE I. Equilibrium distance d_{eq} of the nucleus of the chemisorbed Li from the jellium surface for various Wigner-Seitz radii r_s.

r_s (bohr)	2	3	4
d_{eq} (Å)	1.3	1.0	0.9

tem considered, the stronger the hybridization of the 2*s* and 2*p* states of the Li atom, i.e., the stronger the polarization of the electron cloud around the Li atom.

B. Spatial electron distribution

As described in Sec. II B the change in the electron density in the vicinity of the chemisorbed Li atom can be extracted from the self-consistent calculations. Since the core density of the atom is kept frozen, only a change in the valence electron density $\Delta n(\mathbf{r})$ is possible within the framework of Sec. II B. In Fig. 3 contour plots of $\Delta n(\mathbf{r})$ are shown for chemisorbed atom on the jellium systems $r_s=2$ and $r_s=4$ (bohr). Because of the axial symmetry around the *z* axis, the plane corresponding to $y=0$ is chosen. The vertical axis corresponds to the *z* axis, and the horizontal axis to the *x* axis, respectively. The beginning of the positive background n_+ is marked by a solid line. The unit for the electron density is Å^{-3}.

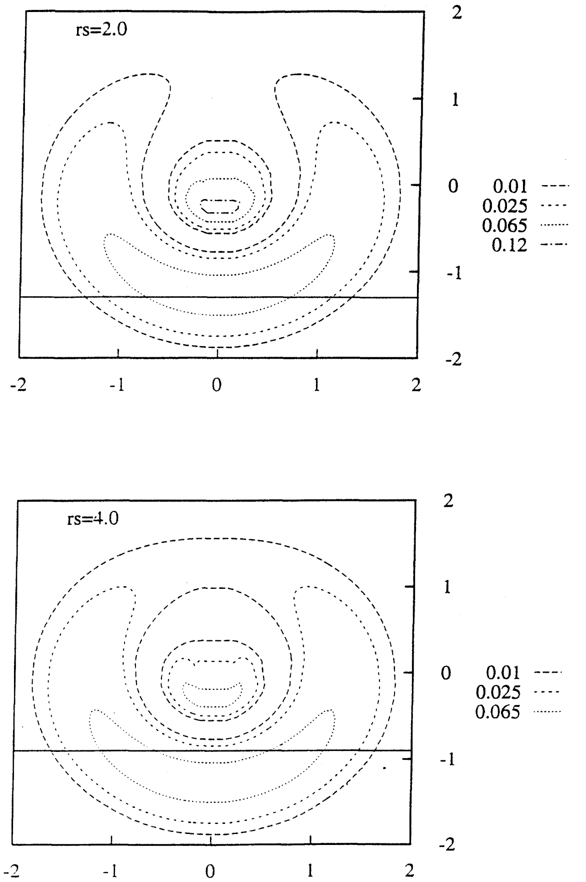

FIG. 3. Two-dimensional cut through the induced spatial electron density for two different r_s and their equilibrium distances. The point (0,0) is the nuclear site, the solid line is the jellium surface. The distribution has rotational symmetry around an axis perpendicular to the surface through the nucleus. Contour lines for several electron densities are plotted.

Both plots show that the density is moved from the vacuum side into the region between the metal surface and the chemisorbed atom. This is the typical result of an isolated atom chemisorbed on a metal surface, since the metal tries to screen out the positively charged ion.[17] However, the magnitude of the polarization of the electron cloud around the atom is different in the two systems. A stronger electronic polarization occurs for the jellium substrate with $r_s=2$ (bohr) in comparison to $r_s=4$ (bohr). This is most clearly seen from the contour level of 0.01 Å^{-3}, which consists of two separate, nearly spherical lines in the case of $r_s=4$ (bohr). In the case of $r_s=2$ (bohr), however, only one closed line is seen at that value of the density showing no extended contribution to the electron density on the vacuum side. Thus the electronic polarization of the Li atom is stronger when adsorbed on a jellium surface with small r_s. Since the smaller the value of r_s the higher the work function, one can conclude that the electron cloud around the Li atom becomes more strongly polarized on substrates with high work functions. This result for the spatial density distribution is consistent with the picture obtained from the induced density of states, discussed in Sec III A (cf. Fig. 2), and in Ref. 19.

C. Relaxation rate

In this section we present results for the nuclear-spin-relaxation rate of a chemisorbed Li atom on different jellium surfaces. Since the magnetic moment of the Li atom enters the equation for the relaxation rate [cf. Eq. (13)], one has to distinguish between the isotopes ^{7}Li and ^{6}Li. The following calculations were performed for the isotope ^{6}Li. Measurements of relaxation rates were performed on *hot* surfaces,[3] the temperature being usually above 1000 K. The calculated relaxation rates are therefore for a temperature of 1000 K. In Fig. 4 the dependence of the relaxation rate α on the work function of different jellium systems is shown. The work function is chosen as the parameter in the system against which the relaxation rate is plotted, since usually experimental data are also plotted in this way. The calculations were performed for values of $r_s=2$, 2.5, 3, 3.5, and 4 (bohr).

From Fig. 4 one infers the following results. First, the value of α lies within the range of 1 s^{-1} and 2 s^{-2}. From NMR measurements relaxation rates are known, which vary from 10^{-3} to 10^3 s^{-1} for different systems (solids, liquids, etc.).[6] According to the present results, the relaxation rates for Li atoms chemisorbed on metal surfaces are expected to be of the order of 1 s^{-1}. As a second result Fig. 4 shows that the relaxation rate becomes smaller with increasing work function of the bare metal system. This behavior of the relaxation rate is connected with the degree of polarization of the electron cloud around the Li atom. As demonstrated in Figs. 2 and 3, the electronic polarization of the Li atom is enhanced for systems with

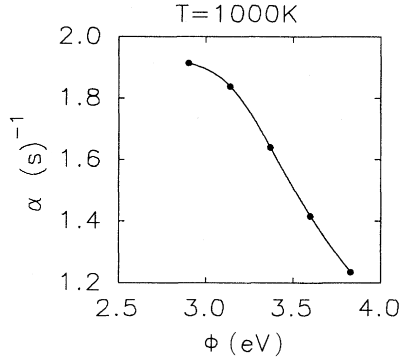

FIG. 4. Nuclear-spin-relaxation rate for Li on a jellium surface as dependent on the work function for a temperature of 1000 K.

high work functions. Thus the LDOS, which is connected to the s part of the wave function, is decreased, resulting in a lower relaxation rate.

In Fig. 5 experimental results of relaxation rates are shown as measured on different metal surfaces.[2,3] Two main features can be noted in this figure. First the data points lie in the range 0.5–2.5 s^{-1}, and, second, the measured relaxation rate shows a clear downward trend with increasing work function. Thus the theoretical results for the relaxation rates calculated in the jellium model correctly predict the order of magnitude of the relaxation rate and its work-function dependence. From these results one can conclude that the Fermi contact interaction describes the dominant process responsible for the nuclear-spin relaxation on metal surfaces.

A more direct comparison of the present results for a jellium substrate with the data was not possible because the present method is poorly suited for work-function values above 4 eV, as test calculations showed. This is consistent with the fact that the jellium model provides a good description only for sp metals which have rather small values for the work functions. For details of the jellium model see Refs. 17 and 18. Therefore the work function within the jellium model vary from 2.5 to 4.0 eV, whereas the experiments were performed on transition metals which have work functions above 4 eV. Presently, measurements on metals with work functions below 4 eV are not practical for technical reasons. The question then arises how the d electrons in the transition metal influence the relaxation rate. Since the d electrons are very localized in space their direct influence at the position of the nucleus should be less important. On the other hand, the relatively narrow energy band of the d electrons means less interaction between the Li atom and the substrate, which should increase the relaxation rate as in the jellium results. Another point should be mentioned here. The jellium model describes the perfect metal, since all electrons are treated as *free* electrons. As a consequence the screening properties of the jellium surface are overestimated in comparison with real metal surfaces. Again looking at the jellium results, the better the screening the smaller the relaxation rate [cf. $r_s=2$ and 4 (bohr)]. Thus one should expect smaller relaxation rates for real metal surfaces as in the corresponding jellium model. The main deficiency in the jellium model is of course the absence of any structure. There is no dependence of the relaxation rate resulting from different adsorption sites due to different surface geometries. In comparison, the experimental data clearly show such a geometric influence of the substrate surface. Therefore the work function is only one substrate parameter relevant to the relaxation rate. Nevertheless, it may be stressed that essential features determining the relaxation rate for the nuclear-spin polarization of atoms chemisorbed on metal surfaces are included in the jellium model.

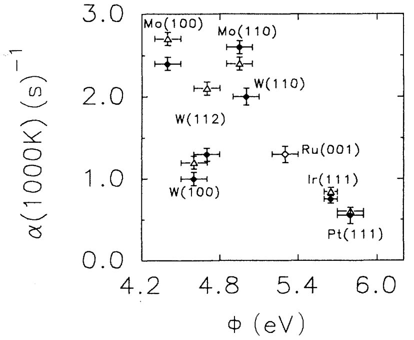

FIG. 5. Data for nuclear-spin-relaxation rates of Li on various surfaces at 1000 K. Data are taken from Ref. 3.

IV. SUMMARY AND CONCLUSION

In this paper we gave a theoretical description of the nuclear-spin relaxation of atoms chemisorbed on metal surfaces. The interaction considered is the Fermi contact interaction. Considering the nuclear-spin relaxation as a dissipative process, a rate equation is derived through methods of statistical physics. As a result the rate of relaxation depends on the local density of states at the position of the nucleus of the Li atom at the Fermi energy.

We discussed the chemisorption of Li atoms on a jellium model surface. Results for the induced density of states, the spatial electron density, and the relaxation rates are presented and discussed. From the induced density of states and the spatial distribution of the electron density, one finds that the Li atom is more polarized the higher the work function of the metal surface. The relaxation rate of the chemisorbed Li atom at 1000-K temperature varies from 1.0 to 2.0 s^{-1}. It decreases with increasing work function of the bare metal surface. Since the relaxation rate is connected to the s part of the wave function, this behavior is consistent with the stronger polarization of the Li atom on metals with high work functions.

The theoretical prediction of the magnitude and the work-function dependence of the relaxation rate of chemisorbed Li atoms is consistent with the experimental results. Thus one can conclude that the Fermi contact interaction is the dominant process responsible for the nuclear-spin relaxation on metal surfaces. Furthermore, it may be concluded that the jellium model for the substrate also gives a good picture in the present context. Further refinements concerning the description of the substrate are necessary in order to cover *d* electrons within the metals and the dependence of the relaxation rate on the crystallographic specification of the surface and the geometric site of the chemisorbed atom.

ACKNOWLEDGMENT

We would like to thank the AG Nukleare Oberflächenphysik in Marburg for providing us with the experimental data shown in this work. We are also grateful to E. Wimmer, D. Fick, H. J. Jänsch, and M. Kaack for many helpful discussions.

---

[*] Present address: Department of Physics and Astronomy, Northwestern University, Evanston, IL 60208.

[1] J. K. Nørskov, Rep. Prog. Phys. **53**, 1253 (1990).

[2] M. Riehl-Chudoba and D. Fick, Surf. Sci. **251/259**, 97 (1991).

[3] M. Kaack and D. Fick (unpublished).

[4] D. Fick, Appl. Phys. A **49**, 343 (1989).

[5] C. P. Slichter, *Principles of Magnetic Resonance* (Springer-Verlag, Auflage, 1989), p. 3.

[6] A. Abragam, *Principles of Nuclear Magnetism* (Oxford University Press, Oxford, 1983).

[7] M. Simonius, in *Polarization Nuclear Physics,* edited by D. Fick, Lecture Notes in Physics Vol. 30 (Springer-Verlag, Berlin, 1974).

[8] G. Schatz and A. Weidinger, *Nukleare Festkörperphysik* (Teubner, Lepizig, 1985).

[9] E. Fick and G. Sauermann, *The Quantum Statistics of Dynamic Processes* (Springer-Verlag, Berlin, 1990).

[10] D. Forster, *Hydrodynamics Fluctuations Broken Symmetry and Correlation Function* (Benjamin, New York, 1975).

[11] P. Hohenberg and W. Kohn, Phys. Rev. B **136**, 864 (1964).

[12] W. Kohn and L. J. Sham, Phys. Rev. A **140**, 1133 (1965).

[13] G. D. Mahan and K. R. Subbaswamy, *Local Density of Polarizability* (Plenum, New York, 1990).

[14] J. P. Perdew and A. Zunger, Phys. Rev. B **23**, 5048 (1983).

[15] M. Scheffler, Ch. Droste, A. F. Leszar, F. Máca, G. Wachutka, and G. Barzel, Physica **172B**, 143 (1991).

[16] N. D. Lang and W. Kohn, Phys. Rev. B **1**, 4555 (1970).

[17] N. D. Lang and A. R. Williams, Phys. Rev. B **18**, 616 (1978).

[18] E. Clementi and C. Roetti, At. Data Nucl. Data Tables **14**, 179 (1974).

[19] W. Mannstadt and G. Grawert (unpublished).